Indian Journal of Chemistry
Vol. 58A, January 2019, pp. 18-28

Investigation of structure-property correlation in 2,2′-dipyridyl diselenide based derivatives

Prasad P Phadnis[a, b,*], Sandeep Nigam[a, b], Ratikanta Mishra[a], Amey Wadawale[a], Mukesh Kumar[c], Amit Kunwar[d], Chiranjib Majumder[a], K I Priyadarsini[a, b] & Vimal K Jain[e]

[a]Chemistry Division, Bhabha Atomic Research Centre, Mumbai 400 085, India

[b]Homi Bhabha National Institute, Anushaktinagar, Mumbai 400 094, India

[c]Radiation Biology & Health Sciences Division, Bhabha Atomic Research Centre, Mumbai 400 085, India

[d]Radiation & Photochemistry Division, Bhabha Atomic Research Centre, Mumbai 400 085, India

[e]UM-DAE Centre for Excellence in Basic Sciences, Health Centre, University of Mumbai, Kalina Campus, Santacruz (E), Mumbai 400 098, India

Email: phadnisp@barc.gov.in

Received 28 August 2018; revised and accepted 18 December 2018

Structure-property correlation in 2,2′-dipyridyl diselenide derivatives has been investigated using four test cases 2,2′-dipyridyl diselenide **(1)**, 2,2′-disleno-bis(3-pyridinol) **(2)**, 2,2′-diseleno-bis(3-carboxypyridine) **(3)** and 2,2′-diseleno-bis (3-nicotinamide) **(4)**. Nature of substituent at C-3 position of pyridyl ring has been found to be a key factor in controlling the molecular structure, its packing capacity and thermal stability of molecular assembly. Strong electron withdrawing group (viz., -COOH, -$CONH_2$) reduces the charge on selenium and enforces sp^2 hybridization induced planar molecular configuration. Bent molecules **1** and **2** favor denser crystallographic packing in comparison to planar molecule **3** and **4**. Thermal investigation reveal that temperature range for thermal decomposition to elemental selenium for **4** and **2** is 210–460 °C and 150–275 °C respectively indicating higher thermal stability of former. The higher thermal stability of **4** has been attributed to secondary intermolecular interactions with the entrapped solvent molecule in the molecular lattice, which is not the case for **2**. The evaluation of these compounds for glutathione peroxidase (GPx) like activity revealed that a stronger electron withdrawing group at C-3 position presented better activity. Thus C-3 position of pyridyl ring of dipyridyl diselenide derivatives can be adopted as one of the focus points for future drug designing processes.

Keywords: 2,2′-Dipyridyl diselenides, Molecular structures, Polymorphism, X-ray structures, Theoretical calculations, Thermal studies

Selenium is an essential micronutrient and exists in the form of selenocysteine in biological systems[1]. Selenocysteine is present at the active sites of several selenoenzymes which exhibit various biochemical roles such as glutathione peroxidase, which is an important antioxidant enzyme[2]. The deficiency of Se is linked with various disease states while its disease preventive and pharmacological role is now accepted. To mimic functions exhibited by selenoenzymes, considerable efforts have been made to develop low-molecular weight organoselenium compounds[1-4]. Attempts have also been made to synthesize organoselenium compounds by incorporating selenium in biologically relevant organic molecules such as pyridinol, nicotinic acid, nicotinamide, etc.[5-11] Several of them have been evaluated for enzyme mimicking activities as well as for their various pharmacological activities. They are also under clinical trials (e.g., ebselen) and are emerging as potential drug molecules[1, 4].

An important aspect that affects efficacy of pharmaceutical drug is polymorphism. Different polymorphs may show different melting points, solubilities, chemical reactivity or stability which in turn controls the pharmaceutical properties, such as dissolution rate and biological activity[12]. Thus, determination of the polymorphism of molecules is of great importance. In drug development, polymorphism of active pharmaceutical ingredients remains a challenge. More than 50% active pharmaceutical ingredients are known to exist in multiple polymorphs and are responsible for differences in many properties[12-14].

Polymorphism is strongly related to intrinsic molecular structure. The relationship between molecular structure and polymorphic crystallization

behavior gives important information for the control of polymorphism. Therefore, understanding the structure-polymorphism correlation is of utmost importance. Even though 2,2′-dipyridyl diselenide derivatives are known as potential drug molecules, molecular structure-property correlation in this class of compounds has not been explored so far. Recently we have synthesised a variety of dipyridyl-diselenide derivatives (**1-4**) (Scheme 1) and evaluated their GPx mimicking catalytic activity and antioxidant activity[5,6]. It was worth noting that substitution of different functional groups on C-3 of pyridyl ring resulted in different molecular geometry (viz., bent and planar configurations) and subsequently different polymorphism/biological activity. Specifically, 2,2′-diseleno-bis(3-nicotinamide) **(4)** has shown gradual depletion of GPx activity with ageing of the sample, although there was no change in the NMR spectra of the aged sample. This indicates that depletion of GPx activity may not be due to molecular structure, but possibly due to transformation into another polymorph on ageing. Thus, performance of 2,2′-dipyridyl diselenide derivatives seem to be heavily dependent on polymorphism. In order to understand the polymorphism and performance of 2,2′-dipyridyl diselenide derivatives, the first step in the molecular designing process, is to understand the connection between molecular structure and property. In view of this, the present work aims to investigate the connection between molecular structure of 2,2′-dipyridyl diselenide derivatives and observed properties of molecular assemblies of 2,2′-dipyridyl diselenide derivatives. For this purpose, four 2,2′-dipyridyl diselenide derivatives having different functional groups on C-3 of pyridyl ring (-H **(1)**, -OH **(2)**, -COOH **(3)** and -$CONH_2$ **(4)**) have been chosen. The selection of these molecules is guided by the fact that they differ in their geometrical arrangements which provides an opportunity to understand structure-property correlation. The 2,2′-diseleno-bis(3-nicotinamide) has been given special attention as it is known to show potent biological activities[6,7]. 2,2′-Diseleno-bis(3-nicotinamide) has been synthesized and analyzed via single crystal XRD and thermal studies. For the remaining three molecules 2,2′-dipyridyl diselenide **(1)**, 2,2′-disleno-bis(3-pyridinol) **(2)** and 2,2′-diseleno-bis (3-carboxypyridine) **(3)**, the data has been taken from our previous work[5-7]. In addition to this, theoretical calculations have also been performed on these molecules to rationalize their structural preference.

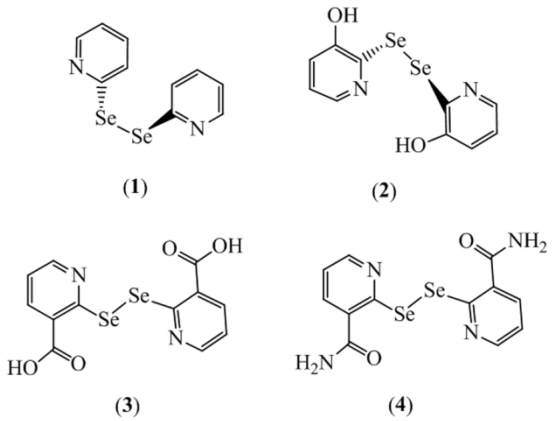

Different molecular geometries viz., bent (**1**, **2**) and planar (**3**, **4**) of dipyridyl- diselenide derivatives

Scheme 1

Materials and Methods

Elemental selenium (99.99%), sodium borohydride and 2-chloro nicotinic acid were purchased from commercial sources (Sigma Aldrich). All reactions were performed under a nitrogen atmosphere. The solvents were purified by standard procedures and were distilled prior to use. The compounds were purified by recrystallization in hot water or polar organic solvents like MeOH, DMF and DMSO, etc. Melting points were determined in capillary tubes and are uncorrected. Elemental analyses were carried out on Flash EA 1112 Series CHNS Analyzer. NMR spectra were recorded on a Bruker Ascend^{TM} 400 MHz spectrometer operating at 400.13 (^{1}H), 100.61 (^{13}C{^{1}H}) and 76.31 MHz (^{77}Se{^{1}H}) in DMSO-d_6. ^{1}H and ^{13}C{^{1}H} NMR chemical shifts are relative to internal DMSO peak. The ^{77}Se{^{1}H} NMR chemical shifts were relative to external Ph_2Se_2 in $CDCl_3$ (δ 463.0 ppm relative to Me_2Se (0 ppm)).

Synthesis of 2-choro-3-nicotinamide

The 2-chloro-3-nicotinic acid was refluxed with thionyl chloride ($SOCl_2$) at 60 ºC for 1 h and then liq. NH_3 was added at the temperature of dry ice (-78 °C). The reaction mixture was stirred for 2 h and the NH_3 was allowed to evaporate at room temperature in a fume hood. The residue was separated on silica gel by column chromatography using chloroform as eluent to yield a white crystalline compound. ^{1}H NMR (DMSO-d_6) δ: 7.47 (d, d), 7.77, 8.06 (each br s, NH_2), 7.88 (d, d), 8.44 (d, d). ^{13}C{^{1}H} NMR (DMSO-d_6) δ: 123.2, 133.4, 137.9, 146.4, 150.2, 167.1 ($CONH_2$) ppm.

Synthesis of diseleno-bis(3-nicotinamide) [2-NC_5H_3(3-$CONH_2$)Se]$_2$ (4)

To an aqueous suspension of elemental Se (0.756 g, 9.577 mmol) in a three-necked round bottom flask, sodium borohydride (0.36 g, 9.577 mmol) was added slowly with stirring resulting into a dark red solution which was refluxed for 30 min. After cooling to room temperature, 2-choro-3-nicotinamide (1.5 g, 9.577 mmol) was added slowly with stirring and the solution was refluxed for 5 h till a yellow colored clear solution was obtained. The solution was filtered in a beaker and allowed to cool whereupon a brown crystalline solid was separated, which was filtered out, washed thoroughly with cold distilled water and dried in vacuo (0.830 g, 43%). The solid comprised of dark brown (selone) and lighter colored (diselenide) crystals which were mechanically separated. The latter was recrystallized from hot methanol in air to give pale brown crystals of diselenide (0.35 g, 18%), m. p. 230 ºC (decomp). X-Ray quality crystals can be obtained by recrystallization from DMF and DMSO. Anal. for $C_{12}H_{10}N_4O_2Se_2$: Calcd: C, 36.02; H, 2.52; N, 14.00%. Found C, 35.46; H, 2.57; N, 14.02%. NMR: ^{1}H NMR (DMSO-d_6) δ: 7.28 (dd, 4.6, 7.6 Hz, 2H), 7.83, 8.33 (each br s, NH_2), 8.15 (d,d, 1.5, 7.8 Hz, 2H), 8.48 (d,d, 1.5, 4.6 Hz, 2H). ^{13}C{^{1}H} NMR (DMSO-d_6) δ: 120.0, 128.3 (C-Se), 135.7, 151.8, 160.3 (C-3, py), 168.6 (CO). ^{77}Se{^{1}H} NMR (DMSO-d_6) δ: 524 ppm.

Synthesis of selone [2-NHC_5H_3(3-$CONH_2$)Se] (5)

The dark brown crystals separated from the above preparation were recrystallized from hot water to give X-ray quality brown crystals of selone, m. p. 215 °C (decomp). NMR: ^{1}H NMR (DMSO-d_6) δ: 7.20 (d, d, 4.5, 5.7 Hz, 1H), 7.95 (br s, 2 H, NH_2), 7.99 (d, d, 1.5, 4.5 Hz, 1 H), 8.40 (d, d, 1.2, 5.7 Hz, 1H), 9.79 (br s, NH) (resonances for a small concentration of diselenide were also noted since selone oxidizes slowly to diselenide). ^{13}C{^{1}H} NMR (DMSO-d_6) δ: 116.3, 138.1, 141.6, 141.7, 142.5, 168.4. ^{77}Se{^{1}H} NMR (DMSO-d_6) δ: 364 ppm.

Thermal analysis

Thermogravimetry and differential thermal analysis (TG-DTA) were carried out on a Setaram TG-DTA Instrument (Model SetSys Evolution)[15]. The differential scanning calorimetry (DSC) studies were performed on a Mettler and Toledo differential scanning calorimeter (Model DSC-1). The mass loss and heat effects were plotted as a function of temperature to monitor the thermal stability of compounds. The test samples were placed in a platinum crucible which was heated at a heating rate of 5 K/min under a flow of argon. For DSC measurements, the temperature and the energy involved in phase transition of the samples were determined. In this case the sample sealed in an aluminium crucible was subjected to thermal cycle at a heating/cooling rate of 5 K/min under the flow of argon.

X-ray crystallography

Single crystal X-ray diffraction data for polymorphs of [2-NC_5H_3(3-$CONH_2$)Se]$_2$ (**4**) and [2-NHC_5H_3(3-$CONH_2$)Se] (**5**) were collected at 293/ 298 ± 2 K on an Agilent Super Nova system with Titan CCD detector using Cu-Kα (λ = 1.54184 Å) radiation so that θ_{max} = 66.97°. The unit cell parameters (Table 1) were determined from 25 reflections measured by a random search routine. ORTEP drawings with numbering scheme and hydrogen bonding are shown in Figs 1-3[16]. The intensity data were corrected for Lorenz, polarization and absorption effects with an empirical procedure[17]. The structures were solved by direct methods using ShelXT (Sheldrick, 2015) and refined by full-matrix least squares methods[18,19]. The non-hydrogen atoms were refined anisotropically. The hydrogen atoms were fixed in their calculated positions.

Theoretical calculations

In order to rationalize the structural preference observed for dipyridyl diselenides (py_2Se_2) and its derivatives, calculations were carried out using ab-initio molecular orbital theory based LCAO approach as implemented in the GAMESS software[20]. Geometry optimization (without any symmetry constraint) was done using the hybrid exchange correlation energy functional commonly known as B3-LYP[21-22]. The notation B3 implies three parameter Becke exchange functional and the LYP indicates correlation functional as described by Lee-Yang-Parr. Standard Aug-ccpVDC basis set were employed for all elements.

Results and Discussion

Synthesis and spectroscopy

Recently we have examined 2,2′-dipyridyl diselenide based derivatives for their therapeutic applications like antioxidant, GPx mimics and radioprotectors[5-7]. There was depletion in GPx activity of 2,2′-dinicotinamide diselenide on ageing (Supplementary Data, Fig. S1). To understand the

Table 1 — Crystallographic and structural refinement data for $[2\text{-}NC_5H_3(3\text{-}CONH_2)Se]_2$ **(4)** and $[2\text{-}NHC_5H_3(3\text{-}CONH_2)Se]$ **(5)**

	$[2\text{-}NHC_5H_3(3\text{-}CONH_2)Se]$	$[2\text{-}NC_5H_3(3\text{-}CONH_2)Se]_2$	
		Crystals from DMF	Crystals from DMSO
Chemical formula	$C_6H_6N_2OSe$	$C_{12}H_{10}N_4O_2Se_2$.2 DMF	$C_{12}H_{10}N_4O_2Se_2$.2 DMSO
Formula weight	201.09	546.35	556.41
Color	yellow	yellow	yellow
Crystal size (mm)	0.73 × 0.27 × 0.17	0.2 × 0.1 × 0.05	0.40 × 0.33 × 0.14
Crystal system/ space group	Monoclinic / $P2_{1/n}$	Orthorhombic / Pbcn	Monoclinic/ $P2_{1/c}$
Cell parameters a (Å)	6.1127 (2)	14.9637(3)	8.5566(2)
b (Å)	9.6032(3)	9.0998(2)	14.3828(3)
c (Å)	11.6092(4)	16.4922(4)	9.4730(2)
α (°)	-	-	-
β (°)	94.657(3)	-	107.202(3)
γ (°)	-	-	-
V (Å^3)	679.23(4)	2245.69(9)	1113.67(5)
Z	4	4	4
D_c (g/cm^3)	1.966	1.616	1.659
μ (mm^{-1})/ F (000)	6.886 / 392	4.433 / 1096	6.160 / 556
Limiting indices	$-7 \le h \le 3$; $-11 \le k \le 11$; $-12 \le l \le 14$	$-18 \le h \le 13$; $-7 \le k \le 10$; $-20 \le l \le 17$	$-10 \le h \le 10$; $-17 \le k \le 12$; $-11 \le l \le 11$
range for data collection	5.988 – 73.147	5.364 - 73.202	5.412 - 73.310
No. of reflections collected	1317	2174	2174
No. of independent reflections	1167	1634	1866
Data/restraints/parameters	1317/ 0/ 92	2174 / 2 / 146	2174 / 0 / 138
R indices [$I > 2\sigma$ (I)]	$R1$ = 0.0714; w$R2$ = 0.1844	$R1$ = 0.0549; w$R2$ = 0.1537	$R1$ = 0.0564; w$R2$ = 0.1502
R indices (all data)	$R1$ = 0.0771; w$R2$ = 0.1954	$R1$ = 0.0758; w$R2$ = 0.2074	$R1$ = 0.0660; w$R2$ = 0.1739
$(\Delta/\sigma)_{max}$	0.000	0.001	0.000
$(\Delta\rho)_{max}$, $(\Delta\rho)_{min}$ (Å^{-3})	1.280 *e* Å^{-3}; -1715 *e* Å^{-3}	0.811 *e* Å^{-3}; -1.249 *e* Å^{-3}	1.828 *e* Å^{-3}; -1.548 *e* Å^{-3}
Goodness-of-fit on F^2	1.128	1.121	1.074

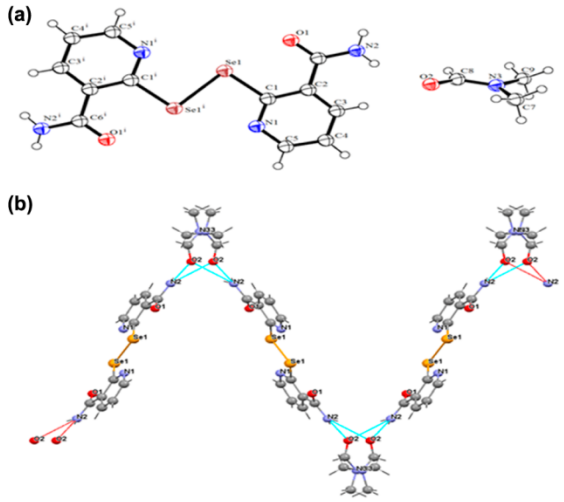

Fig. 1 — (a) Molecular structure of $[2\text{-}NC_5H_3(3\text{-}CONH_2)Se]_2$.2DMF, recrystallized from dimethylfomamide and (b) hydrogen bonding interactions in the structure of $[2\text{-}NC_5H_3(3\text{-}CONH_2)Se]_2$.

reason, we have reinvestigated its synthesis and tried to study its structure property correlation by comparing with other 2,2′-dipyridyl diselenide based derivatives (**1-3**). Hence the compound, $[2\text{-}NC_5H_3(3\text{-}CONH_2)Se]_2$ **(4)** was synthesized according to reported method (Scheme 2) which gave a mixture of diselenide **(4)** and selone **(5)**[6]. The two were separated from water rather than extraction from chloroform, which has helped in improving the yield. Diselenide **(4)** and selone **(5)** were mechanically separated and again recrystallized. The selone can be converted to diselenide by aerial oxidation in methanolic solution. Recrystallization of diselenide from DMF and DMSO gave orthorhombic ($\mathbf{4}_{\mathbf{ortho}}$) and monoclinic ($\mathbf{4}_{\mathbf{mono}}$) forms, respectively.

The ^{1}H, ^{13}C and ^{77}Se NMR spectra exhibited expected resonances (Fig. S2). Samples of selone **(5)** can undergo aerial oxidation to diselenide which is detectable by ^{77}Se NMR (Fig. S3). The ^{77}Se NMR spectra of both selone **(5)** (364 ppm) and diselenides **(4)** (524 ppm) are significantly deshielded from those reported for 3-hydroxy pyridine-2-(1H) selone (156 ppm)[8], 2-pyridyl selone (314 ppm)[23], 2,2′-diseleno-bis

(3-pyridinol) (389 ppm)[24], 2,2′-dipyridyl diselenide (447 ppm)[5], and 2,2′-dipyrimidyl diselenide (490 ppm)[5]. The ^{77}Se NMR chemical shifts of selones and diselenides appear in two distinctly broad ranges and are influenced by the nature of organic group and the presence of secondary interactions.

Crystallography

2,2′-Diseleno-bis(3-nicotinamide) **(4)** on crystallization from DMF and DMSO gave orthorhombic (**4**$_{ortho}$) (Fig. 1) and monoclinic (**4**$_{mono}$) (Fig. 2) forms, respectively. We have isolated crystals of **4** from DMF in the orthorhombic form (**4**$_{ortho}$) whereas Feng *et al.*[25] obtained a triclinic form from DMF. Polymorphism in pyridyl diselenides, such as 2,2′-dipyridyl diselenide (orthorhombic[26] and monoclinic[27]) and 2,2′-diseleno-bis(3-prydinol)[24], has been reported in literature. The Se-Se distances in both the polymorphs of **1** are similar (~2.40 Å) (Table 2) and are significantly longer than those reported for various pyridyl diselenides, like 2,2′-dipyridyl diselenide (~2.29 Å)[26, 27], 4, 4′-dimethyl-2,2′-dipyridyl diselenide (2.2973 (7) Å)[28] and [2-C_5H_3N(3-OH)Se]$_2$ (2.2858(18)–2.3254(11) Å)[24], but can be compared with [2-NC_5H_3(3-CONHPh)Se]$_2$ (2.3916 Å)[6] and [2-NC_5H_3(3-

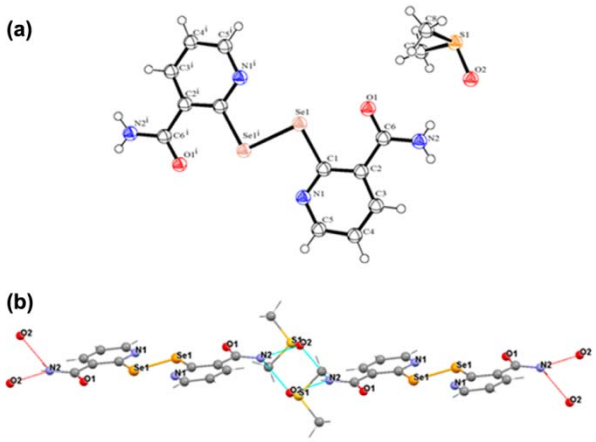

Fig. 2 — (a) Molecular structure of [2-NC_5H_3(3-$CONH_2$)Se]$_2$.2DMSO, recrystallized from dimethylsulfoxide and (b) hydrogen bonding interactions in the structure of [2-NC_5H_3(3-$CONH_2$)Se]$_2$.

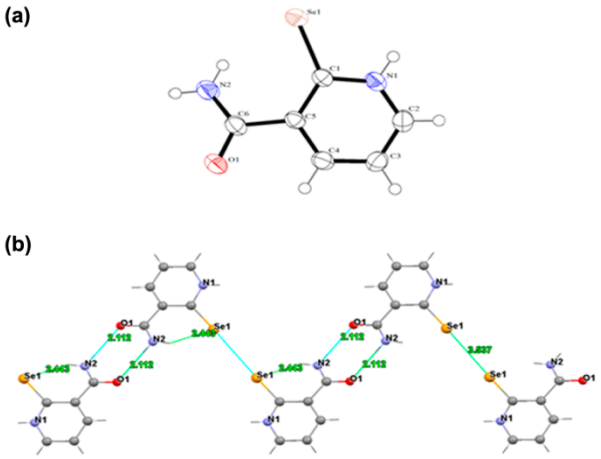

Fig. 3 — (a) Molecular structure of [2-NHC_5H_3(3-$CONH_2$)Se] **(5)** recrystallized from hot water (selected bond lengths (Å) : C1-Se1, 1.858(3); C1-N1, 1.367(4); C2-N1, 1.352(5); C6-O1, 1.231 (**(5)**; C6-N2, 1.322**(6)**; and bond angles (º): N1-C1-Se1, 115.8(2); C5-C1-Se1, 129.3(3); O1-C6-N2, 122.0(3), and, (b) hydrogen bonding interactions in the structure of [2-NHC_5H_3(3-$CONH_2$)Se].

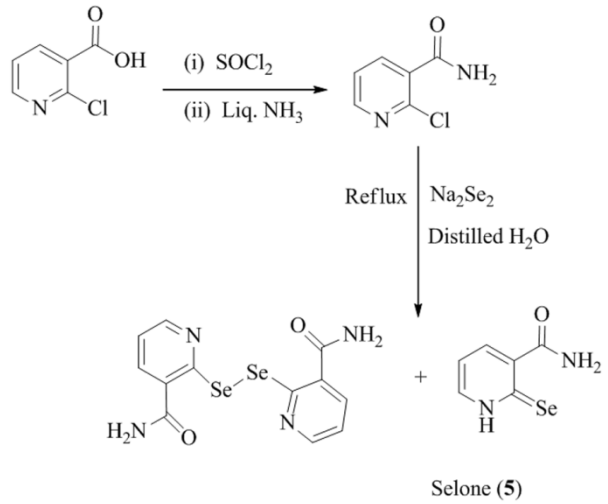

Dinicotinamide diselenide **(4)**

Synthesis of 2, 2′- diseleno-3-dinicotinamide **(4)** and its selone **(5)** analogue

Scheme 2

Table 2 — Selected interatomic parameters (Å/ °) for [2-NC_5H_3(3-$CONH_2$)Se]$_2$

	Crystallized from DMF	Crystallized from DMSO
	Bond lengths (Å)	
Se1-Se1^{i}	2.4001(11)	2.3974(8)
C1-Se1	1.932(6)	1.923(4)
C1-N1	1.321(7)	1.341(6)
C6-N2	1.325(8)	1.315(7)
C6-O1	1.237(7)	1.236(6)
	Bond angles (º)	
C1-Se1-Se1^{i}	92.31(16)	93.07(13)
N1-C1-Se1	115.6(4)	115.8(3)
C2-C1-Se1	121.1(4)	121.5(3)
C2-C6-N2	118.4(5)	118.2(4)
C2-C6-O1	119.6(5)	119.5(4)

$CONH_2)Se]_2$ (2.3877(7) Å)[26]. However, the Se-Se bond distances in $\mathbf{4}_{\mathbf{ortho}}$ and $\mathbf{4}_{\mathbf{mono}}$ are the longest among all the diorganodiselenides. The C-Se-Se angle and C-Se-Se-C torsion angles in $\mathbf{4}_{\mathbf{ortho}}$ and $\mathbf{4}_{\mathbf{mono}}$ are ~93° and 180°, respectively and are similar to $[2\text{-}NC_5H_3(3\text{-}CONHPh)Se]_2$[6] and $[2\text{-}NC_5H_3(3\text{-}CONH_2)Se]_2$ which are similar with the structure reported by Feng *et al*.[25] these angles for 2,2′-dipyridyl diselenide and $[2\text{-}C_5H_3N(3\text{-}OH)Se]_2$ are 102.8(2)°[27] and ~104°[24] respectively. The **4** is almost planar, with only the amide group atoms O1 and N1 being slightly out of the molecular mean plane (0.140 and 0.184 respectively). The distances N1---Se1' (2.868 Å) and O1---Se1 (2.636 Å) (Figs **1**a, **2**a) are longer than the Se-N bond (2.291Å)[29] and Se-O bond (2.21534 Å)[30] reported earlier but are significantly shorter than the sum of the van der Waal radii of the respective atoms, suggesting strong intra-molecular interactions.

In order to understand the connection between the molecular structure and its pattern of assembling/packing, the crystal structure of 2,2′-diseleno-bis(3-nicotinamide) **(4)** (Figs S4 and S5) has been compared with crystal structures of other diselenide derivatives i.e., 2,2′-dipyridyl diselenide (**1**), 2,2′-disleno-bis(3-pyridinol) **(2)** and 2,2′-diseleno-bis(3-carboxypyridine) **(3)**. It is noticed that 2,2′-dipyridyl diselenide **(1)**, 2,2′-disleno-bis(3-pyridinol) **(2)** have bent molecular structure, while 2,2′-diseleno-bis(3-carboxypyridine) **(3)** have planar molecular structure. The bent molecules 2,2′-dipyridyl diselenide **(1)** and 2,2′-disleno-bis(3-pyridinol) **(2)** assemble in monoclinic form with packing density around 2 g cm^{-3}, however planar molecules 2,2′-diseleno-bis(3-carboxypyridine) **(3)** assemble and 2,2′-diseleno-bis(3-amidopyridine) **(4)** with packing density around 1.6–1.7 gcm^{-3} as presented in Table 3. Thus it can be inferred that bent molecules have denser packing compared to their planar counterparts.

The packing of dipyridyl diselenide molecules depends on (i) intrinsic molecular structure and (ii) the intermolecular interaction with solvents/dipyridyl diselenide involved in the packing. Keeping this in mind, the secondary interactions in 2,2′-diseleno-bis(3-nicotinamide) **(4)** were investigated. Both the polymorphs $\mathbf{4}_{\mathbf{ortho}}$ and $\mathbf{4}_{\mathbf{mono}}$ show secondary hydrogen bonding interactions with the lattice solvent molecules (Supplementary Data, Tables S1 and S2). Individual molecules in $\mathbf{4}_{\mathbf{ortho}}$ are hydrogen bonded to two DMF molecules through the amide N2 hydrogen and carbonyl oxygen O2; each DMF carbonyl O2 also interacts with amide N2 hydrogen of two different molecules forming a sinusoidal strand (Fig. 1b). Additionally, there are lateral weak inter-molecular interactions between carbonyl oxygen O1--- aromatic hydrogen H5 linked with C5 (2.550 Å), and pyridyl nitrogen N1--- aromatic H4 linked to C4 (2.647 Å) of adjacent molecule (Supplementary Data, Fig. S2 and Fig. 1b). Both hydrogen bonding and lateral weak intermolecular interactions lead to the formation of a 3D sinusoidal folded super-molecular assembly (Fig. 1b). The major difference between the present $\mathbf{4}_{\mathbf{ortho}}$ and the earlier reported triclinic form by Feng et al.[25] is that in the present case each of the amide groups are identically hydrogen bonded to two DMF molecules, whereas in the triclinic form, both the amide groups are H-bonded differently. One of the amides is hydrogen bonded to two DMF molecules while the other amide group forms an inter-molecular hydrogen bond with amide group of neighboring diselenide molecule in addition to two DMF molecules (Fig. S6). This difference leads to a completely different crystal packing despite the presence of sinusoidal pattern in both; this is due to the hydrogen bonding between diselenide molecules. The $\mathbf{4}_{\mathbf{ortho}}$ has highly ordered H-bonded single sinusoidal strands linked to others through weak inter-molecular interactions whereas in the triclinic form, a 3D network is formed due to the presence of extra H-bond. Individual diselenide molecules in $\mathbf{4}_{\mathbf{mono}}$ are hydrogen bonded to the DMSO molecules (Fig. 2b) leading to the formation of one-dimensional strands which in turn are bonded to

Table 3 — The crystal structural features with secondary interactions influencing the thermal properties of 2,2′-dipyridyl diselenide derivatives

2,2′-dipyridyl diselenide derivatives	Density D_c (g/cm^3) (room temperature) Monoclinic crystal system	Melting Point (°C)	Reference
H **(1)**	1.912	49 °C	5
OH **(2)**	2.034 (in MeOH-H_2O)	185 °C (Lit. 226–227 °C) with phase change at 180–190 °C	24
COOH **(3)**	1.706 (in DMSO)	218-220 °C decomp.	6
$CONH_2$ **(4)**	1.659 (in DMSO)	230 °C decomp.	Present work

the adjacent strands through weak intermolecular forces (Supplementary Data, Fig. S4c) between the aromatic hydrogen C4(H4) and C5(H5) with pyridyl nitrogen N1 and carbonyl oxygen O1, respectively as a consequence a folded sheet like packing structure (Fig. S6) is formed. The difference between $\mathbf{4}_{\mathbf{ortho}}$ and $\mathbf{4}_{\mathbf{mono}}$ is that in the former, DMF bonded diselenide molecules are folded through the solvent molecules whereas in the latter are folded through the intermolecular weak interactive forces (Fig. S7).

From the above discussion, it is clear that 2,2′-diseleno-bis(3-nicotinamide) **(4)** show secondary interaction with the solvent molecules, however no intermolecular hydrogen bonding is found between two 2,2′-diseleno-bis(3-nicotinamide) **(4)** molecules. This observation contrasts with the packing 2,2′-disleno-bis(3-pyridinol) **(2)**, where significant intermolecular hydrogen bonding between two 2,2′-dipyridyl diselenide molecule is observed. This can be attributed to the fact that bent geometry of 2,2′-disleno-bis(3-pyridinol) **(2)** facilitates closer approach and interlocking through intermolecular O-H/N hydrogen binding between two neighboring 2,2′-disleno-bis(3-pyridinol) **(2)** molecules.

However, for 2,2′-diseleno-bis(3-nicotinamide) **(4)** molecule, even though it has the possibility of secondary intermolecular hydrogen bonding, the planar geometry directs the packing of molecule in a fashion where it is difficult to achieve intermolecular hydrogen bonding interaction between two 2,2′-diseleno-bis(3-nicotinamide) **(4)** molecules. Due to the lack of functional group, 2,2′-dipyridyl diselenide **(1)** cannot show any hydrogen bonding. In case of 2,2′-diseleno-bis(3-carboxypyridine) **(3)** also the planar geometry deters the closer packing and hydrogen bonding between two 2,2′-diseleno-bis (3-carboxypyridine) molecules **(3)**.

The X-ray analysis of selone **(5)** revealed that there are two independent molecules of planar pyridine-2(1H)-selone tautomer in the unit cell, which are connected via N-H---O hydrogen bonds (2.112 Å) of the amide group (Table S3). The resulting dimer is distinctly different from the dimer of 2-pyridine selone which exhibits $N_{pyridine}$-H---Se hydrogen bonds[23]. Contrary to these dimeric selones, the selone $C_5H(4,5\text{-}CH_2OH)_2$ (3-OH)NH^+Se^- is a discrete monomer with intramolecular 3-O-H---Se hydrogen bond[8]. Selenium in **5** forms an intra-molecular hydrogen bond with amide proton (2.443 Å) which is significantly shorter than the sum of van der Waals radii of selenium and hydrogen atoms (3.10 Å)[31]. Each dimer is interconnected to the adjacent dimer through intermolecular Se---Se (3.537Å) resulting in an infinite chain (Fig. 3). The C-Se distance (1.858(3) Å) is intermediate between C-Se single bond (1.94 Å) and C=Se double bond (1.74 Å), indicating resonance stabilized C=Se double bond[8, 23].

Thermal Studies

The TG-DTG plot (Fig. S8) of 2,2′-diseleno-bis(3-nicotinamide) **(4)** recrystallized from hot methanol shows mass loss in four successive steps. The initial mass loss (~1%) observed in the temperature range 25–130 °C is assigned to loss of adsorbed solvent from the sample. The mass loss (36%) in the first step (210–300 °C) can be attributed to the loss of one nicotinamide and NH_2 fragment (calculated mass loss 34%). The mass loss in the second (mass loss 15% at 300–388 °C) and third stage (mass loss 9% at 388–460 °C) can be associated with the elimination of organic residues leaving behind elemental selenium which tends to vaporize above 460 °C. Corresponding DSC plot has been shown in Supplementary Data, Fig. S9.

The comparison of thermal decomposition of 2,2′-diseleno-bis(3-nicotinamide) **(4)** with previously reported 2,2′-disleno-bis(3-pyridinol) **(2)** has been presented in Fig. 4[24]. Comparison of the two revealed that 2,2′-disleno-bis(3-pyridinol) **(2)** molecular assembly decomposes to elemental selenium in the temperature range 150–275 °C, while 2,2′-diseleno-bis(3-nicotinamide) **(4)** molecular assembly decomposes to elemental selenium in the temperature range 210–460 °C. The higher thermal stability of **4** molecular assembly, is attributed to the presence of strong secondary interactions of **4** with solvent molecules entrapped in the lattice. Such interactions are not present in case of 2,2′-disleno-bis(3-pyridinol)

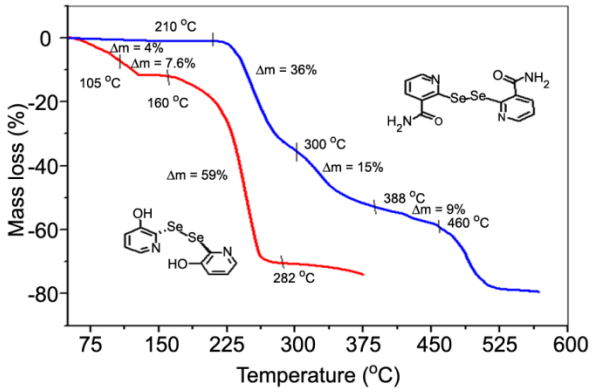

Fig. 4 — Comparison of thermal behavior of [2-C_5H_3N(3-$CONH_2$)Se]$_2$ **(4)** and [2-NC_5H_3(3-OH)Se]$_2$ **(2)** (data for **2** are from Ref 24).

(2). In other words, secondary hydrogen bonding interactions between two dipyridyl diselenide derivatives are weaker than the interactions between a dipyridyl diselenide derivative and solvent molecule.

Theoretical study

The structures of several substituted 2,2′-dipyridyl diselenides have been reported. Planarity (C-Se-Se-C torsion angles) of a molecule is greatly influenced by the nature of the substituents and their position in the pyridyl ring. Unsubstituted pyridyl ring[26,27], and the ring substituted at 3-position by an electron releasing group (e.g., 3-Me (87.90º)[32]) results in an angular structure whereas the ring substituted at 3-position by an electron withdrawing group (e.g., Br[33], CF_3[34], COOH[35], $COOBu^t$ [35b], $CONH_2$[25], CONHPh[6], $CONMe_2$[36]) leads to a planar molecule, with the exception of bis(3-hydroxy-2-pyridyl) diselenide (93.04, 94.21°)[24]. The substituents at other positions in the pyridyl ring, irrespective of their nature (electron releasing or withdrawing) (e.g., 4-Me (89.29°)[29], 4-NMe_2 (73.75°)[37], 5-CF_3 (83.36°)[34], 6-Me (89.76°)[38]), invariably produce angular structures. In di- and higher substituted derivatives, when 3-position in the ring is substituted (e.g., bis(3,6-dimethylpyridin-2-yl) diselenide (180º)[39], di{6-bromo-4,5-bis(carboxylethyl)-3-hydroxyl-2-pyridyl} diselenide (178.08º)[9]) planar structures are formed whereas when C-3 position of the ring is unsubstituted (e.g., bis(5,6-dimethylpyridin-2-yl) diselenide (81.97°)[40]) angular structures are formed. Clearly, the structures of 2,2′-dipyridyl diselenide and its derivatives depend on the substituent present at C-3 position of pyridyl ring as observed from experimental data. In order to understand the reasoning behind this, theoretical calculations were carried out on the dipyridyldiselenide derivatives (**1-4**). The calculated geometrical parameters (bond lengths and bond angles) showed good agreement with those obtained from X-ray crystallographic data. 2,2′-Dipyridyl diselenide **(1)** and 2,2′-diseleno-bis (3-pyridinol) **(2)** favors bent structure, while corresponding nicotinoyl derivatives i.e., 2,2′-diseleno-bis(3-carboxypyridine) ($[2\text{-}NC_5H_3(3\text{-}COOH)Se]_2$ **(3)** and 2,2′-diseleno-bis(3-nicotinamide) ($[2\text{-}NC_5H_3(3\text{-}CONH_2)Se]_2$ **(4)** adopt a planar structure (Table 4). Other low-lying isomers are presented in Fig. S10.

The py_2Se_2 derivatives with bent geometry [i.e., 2,2′-dipyridyl diselenide and 2,2′-disleno-bis(3-pyridinol)] (**3**) have shorter Se-Se bonds than those molecules which have a planar configuration [i.e., 2,2′-diseleno-bis(3-nicotinamide) and 2,2′-diseleno-bis(3-carboxypyridine)]. It is worth noting that average positive charge on Se atom (Lowdin charge) is more for planar molecules than those with bent structures. The relative positive character of selenium is also manifested in ^{77}Se NMR chemical shifts which appear ~350 ppm for bent molecules whereas for planar compounds they lie ~500 ppm. The compounds 2,2′-diseleno-bis(3-nicotinamide) and 2,2′-diseleno-bis(3-carboxypyridine) also exhibit intramolecular non-bonding interactions between selenium and oxygen atom of the carbonyl group as the distance between these atoms is less than that of the sum of their van der Waals radii.

Table 4 — Geometry and Se charge of 2,2`-dipyridyl diselenide derivatives

Molecule	2,2′-dipyridyl diselenide**(1)**	2,2′-disleno bis (3-pyridinol)**(2)**	2,2′-diseleno-bis (3-carboxypyridine)**(3)**	2,2′-diseleno-bis (3-nicotinamide)**(4)**
Structure	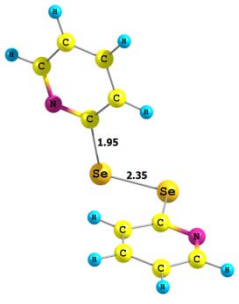	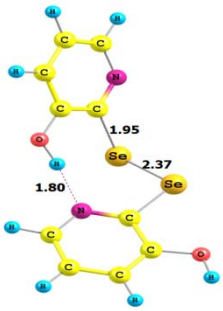	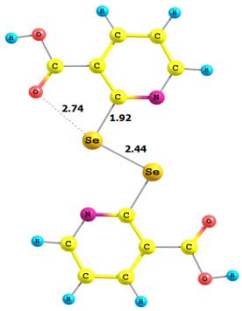	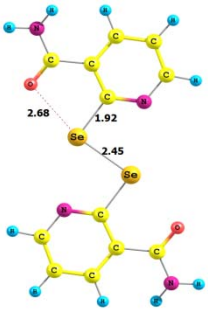
Lowdin charge on each Se	+0.57e	+0.57e	+0.69e	+0.70e
^{77}Se NMR chemical shift (in ppm)	347.0	387.5	506.0	525.7
Se-N-C2 bond angle (in °)	120.2	120	116.4	116.7
Se-Se bond distance (in Å)	2.35	2.37	2.44	2.45

The frontier molecular orbitals of py_2Se_2 derivatives are shown in Fig. 5 whereas other MOs are given in Supplementary Data, Fig. S11. In all diselenides, the highest occupied molecular orbital (HOMO) is localized primarily on selenium atoms. For the planar molecules (X = -COOH, $CONH_2$); the HOMO-1 and HOMO has the character of π(Se-Se) and π*(Se-Se) orbitals respectively made by p_z orbitals of Se atoms. However, for the molecules with X = -H, OH, the HOMO-1 and HOMO have cross overlaps of p_z orbitals of two Se atoms owing to bent geometry. To get further insight about geometrical influence on the molecular orbital shape, a detailed analysis of molecular orbital of planar and bent isomers of representative 2,2′-dipyridyl diselenide was carried out. Contribution of Se atom in various molecular orbitals in planar and bent geometries is given in Supplementary Data, Table S4. As is evident from Table S4, the molecular orbital in planar isomer of 2,2′-dipyridyl diselenide can be loosely approximated as sp^2 hybrid orbitals with s, p_x and p_y orbitals of Se atom and p_z orbital that remains distinct and appears in HOMO-1 and HOMO. However, for the bent isomer of the same molecule, the p_z orbital does not remain distinct and combines with other orbitals (viz. Ψ_{66}, Ψ_{67}, Ψ_{69} and Ψ_{70} molecular orbitals in Table S4) leading to deviation from the sp^2 hybridization. It is worth mentioning that in planar isomer of 2,2′-dipyridyl diselenide has more positive charge on the Se atoms in comparison to the bent counterpart. Thus, it can be inferred that removal of charge from the Se atoms helps p_z orbital to remain discrte and this in turn favors sp^2 hybridization at Se atoms with planar geometry. Isolation of p_z orbital from the surrounding orbital leads to decrease in the bond order of Se-Se bond which is in consonance with elongated Se-Se bonds for planar molecules. Clearly the charge on Se in a diselenide strongly influences its geometry and electronic structure. In order to confirm the effect of charge on the geometrical aspect, additional calculations for 2,2′-dipyridyl diselenide were carried out after removing one electron from the corresponding neutral molecule. It was found that when the electron is removed from the HOMO of the neutral molecule, the relative stability order of the geometrical isomers is reversed (Table 5). Similar behavior was also observed for 2,2′-disleno-bis(3-pyridinol) **(2)**.

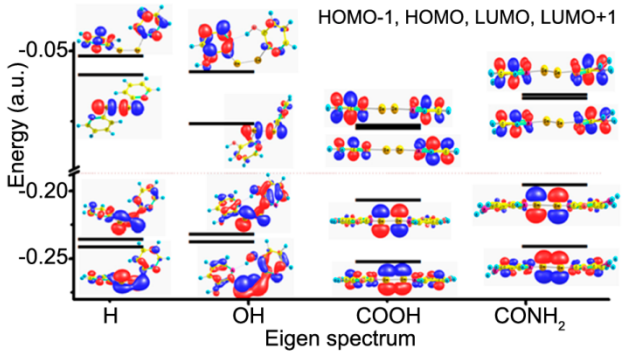

Fig. 5 — Frontier molecular orbitals of py_2Se_2 derivatives.

Additionally, py_2Se_2 derivatives with bent geometry [i.e. 2,2′-dipyridyl diselenide and 2,2′-disleno-bis(3-pyridinol)] have lowest unoccupied molecular orbital (LUMO) localized on selenium atoms. However, for planar 2,2′-diseleno-bis(3-carboxypyridine) **(3)** and, 2,2′-diseleno-bis(3-nicotinamide) **(4)** LUMO is confined mainly on the pyridine ring without any contribution from Se atoms. Gamez and co-workers reported that in case of XSeSeX` diselenides, when X is a substituent with low electronegativity, the LUMO is constituted by σ*(Se-Se) antibonding orbital[40]. But when X is a highly electronegative substituent, σ*(Se-X) bond becomes highly stabilized with respect to σ*(Se-Se) antibonding orbital favoring σ*(Se-X) orbital as LUMO and Se-Se remains uninvolved. Similar to this, in the present case, substitution with strong electron withdrawing group (viz. -COOH, $-CONH_2$) reduces the electron density at Se atom, which leads to a LUMO which does not have contribution from Se-Se bonds. Hence these observations further confirm the influence of Se charge on electronic structure of py_2Se_2 derivatives.

Table 5 — Effect of Se charge on geometrical isomers of 2,2′-dipyridyl diselenide derivatives

	Total Energy (a.u.) Neutral molecule $[py_2Se_2]$	Total Energy (a.u.)[a] Cation $[py_2Se_2]^+$
2,2′-dipyridyl diselenide (bent isomer)	–5297.9938962	–5297.7164357
2,2′-dipyridyl diselenide (planar isomer)	–5297.9857269	–5297.7290353
2,2′-diseleno-bis (3-pyridinol) (bent isomer)	–5448.4092576	–5448.1113970
2,2′-diseleno-bis (3-pyridinol) (planar isomer)	–5448.3952872	–5448.1361401

[a]one electron removed, keeping the same geometrical arrangement

From the foregoing discussion it is clear that the nature of substituent at C-3 position of pyridyl ring in 2,2′-dipyridyl diselenide strongly influences the geometry and electronic structure of the molecule. Presence of strong electron withdrawing group (viz., -COOH, -$CONH_2$) favors planar configuration of py_2Se_2 over the bent one. The preference for planar geometry has been attributed firstly to the reduction of electron density at Se atom which allows p_z orbital of Se atom to remain distinct from its nearby orbitals and secondly, more positive charge on Se atoms allows it to participate in non-bonding interactions with oxygen atom of carbonyl group of $COOH/CONH_2$. In previous sections, it is found that bent and planar molecular nature is directing the packing pattern as well as the thermal stability. Therefore, in totality one can say that the nature of substituent at C-3 position of pyridyl ring in 2,2′-dipyridyl diselenide is governing the packing pattern and thermal stability via two functionalities i.e., (i) by controlling the charge on Se and hence the molecular geometry and (ii) by controlling the secondary interactions with nearby molecules.

Conclusions

Structure-property correlation in 2,2′-dipyridyl diselenide (**1**), 2,2′-disleno-bis(3-pyridinol) **(2)**, 2,2′-diseleno-bis(3-carboxypyridine) **(3)** and 2,2′-diselenobis(3-nicotinamide) **(4)** has been investigated. The nature of substituent at C-3 position of pyridyl ring in 2,2′-dipyridyl diselenides play a key factor in governing the molecular structure (bent versus planar), molecular packing/thermal stability via controlling (i) charge on selenium atoms and (ii) secondary interactions with nearby molecules respectively. Presence of strong electron withdrawing group (viz., -COOH, -$CONH_2$) favors planar configuration of py_2Se_2 derivatives over the bent one. Further it is found that intrinsic molecular structure of 2,2′-dipyridyl diselenide derivative dictates the crystallographic packing of these molecules. The bent molecules 2,2′-dipyridyl diselenide (**1**), 2,2′-diseleno-bis(3-pyridinol) **(2)** assemble with packing density around 2 g cm^{-3}, however planar 2,2′-diseleno-bis (3-carboxypyridine) **(3)** and 2,2′-diseleno-bis(3-nicotinamide) **(4)** assemble with packing density around 1.6–1.7 g cm^{-3}. The glutathione peroxidase (GPx) like activities revealed the direct relation of stronger electron withdrawing group at C-3 position with better activity.

Supplementary data

Crystallographic data for the structural analyses have been deposited with the Cambridge Crystallographic Data Centre under CCDC Nos. 1570318, 1570317 and 1570319 for selone, diselenide crystallized from DMSO and diselenide crystallized from DMF, respectively. Copies of this information may be obtained free of charge from: The Director, CCDC, 12 Union Road, Cambridge CB2 1EZ, UK (fax: (int. code) +44 1223-336-033; e-mail: deposit@ccdc.cam.ac.uk or www: http://www.ccdc.cam.ac.uk). Other supplementary data associated with this article are available in the electronic form at http://www.niscair.res.in/jinfo/ijca/IJCA_58A(01)18-28_SupplData.pdf.

References

1 Jain V K & Priyadarsini K I, *Organoselenium compounds in biology and medicine: Synthesis, biological and therapeutic treatments*, (RSC, Cambridge, UK), 2018.

2 (a) Mugesh G, DuMont W W & Sies H, *Chem Rev*, 101 (2001) 2125; (b) Bhabak K P & Mugesh G, *Acc Chem Res,* 43 (2010) 1408.

3 Nogueira C W, Zeni G & Rocha J B T, *Chem Rev*, 104 (2004) 6255.

4 Santi C, *Organoselenium Chemistry: Between synthesis and biochemistry*, (Bentham Science Publishers), 2014.

5 Hodage A S, Prabhu C P, Phadnis P P, Wadawale A & Priyadarsini K I, *J Organomet Chem*, 720 (2012) 19.

6 Prabhu C P, Phadnis P P, Wadawale P P, Priyadarsini P P & Jain V K, *J Organomet Chem*, 713 (2012) 42.

7 Prabhu P, Singh B G, Noguchi M, Phadnis P P, Jain V K, Iwaoka M. & Priyadarsini K I, *Org Biomo. Chem*, 12 (2014) 2404.

8 Singh V P, Poon J, Butcher R J & Engman L, *Chem Eur J*, 20 (2014) 12563.

9 Singh V P, Poon J, Butcher R J, Lu X, Mestres G, Ott M K & Engman L, *J Org Chem*, 80 (2015) 7385.

10 Moreno E, Plano D, Lamberto I, Font M, Encio I, Palop J A & Samartin C, *Eur J Med Chem*, 47 (2012) 283.

11 Dhau J S, Singh A, Singh A, Sharma N, Brandão P, Félix V, Singh B & Sharma V, *RSC Adv*, 5 (2015) 78669.

12 Karpinski P H, *Chem Eng Technol*, 29 (2006) 233.

13 Raza K, Kumar P, Ratan S, Malik R & Arora S, *SOJ Pharm Phar Sci*, 1 (2014) 1.

14 Li H, Kiang Y H & Jona J, *Eur J Pharm Sci*, 38 (2009) 426.

15 (a) Plano D, Lizarraga E, Palop J A & Sanmartín C, *J Therm Anal Cal*, 98 (2009) 559; (b) Plano D, Palop J A & Sanmartín C, 'Thermal Analysis of Sulfur and Selenium Compounds with Multiple Applications, Including Anticancer Drugs', in *Applications of Calorimetry in a Wide Context-Differential Scanning Calorimetry, Isothermal Titration Calorimetry and Microcalorimetry*, chapter 16, edited by A A Elkordy (InTech publishers) (2013); ISBN 978-953-51-0947-1.

16 Johnson C K, ORTEP II, Report ORNL-5136, Oak Ridge National Laboratory, Oak Ridge, TN 1976.

17 CrysAlisPro 1.171.38.41 (Rigaku Oxford Diffraction, 2015).

18 Sheldrick G M, SHELXT – Integrated space-group and crystal-structure determination, *Acta Cryst A*, 71 (2015) 3.

19 Sheldrick G M, Crystal structure refinement with SHELXL; *Acta Cryst C*, 71 (2015) 3.

20 SchmidtW, Baldridge K K, Boatz J A, Elbert S T, Gordon M S, Jensen J H, Koseki S, Matsunaga N, Nguyen K A, Su J S, Windus T L, Dupuis M & Montgomery J A, *J Comput Chem*, 14 (1993) 1347.

21 Becke A D, *Phys Rev A*, 38 (1988) 3098.

22 Lee C, Yang W & Parr R G, *Phys Rev B*, 37 (1988) 785.

23 Laube J, Jäger S & Thöne C, *Eur J Inorg Chem*, (2001) 1983.

24 Phadnis P P, Kunwar A, Kumar M, Mishra R, Wadawale A, Priyadarsini K I & Jain V K, *J Organomet Chem*, 852 (2017) 1.

25 Feng A, Xu Y & Wei X, *Acta Crystallogr, Sect.E: Struct Rep Online*, 66 (2010) o1216.

26 Dunne S, von Nagy-Felsobuki E & Mackay M, *Acta Cryst C*, 54 (1998) 887; Romero J, Duran M L, Garcia-Vazquez J A, Castineiras A, Sousa A, Christiaens L & Zubieta J, *Inorg Chim Acta*, 255 (1997) 307.

27 Kienitz C O, Thöne C & Jones P G, *Inorg Chem*, 35 (1996) 3990.

28 Bhasin K K & Singh J, *J Organomet Chem*, 658 (2002) 71.

29 Kulcsar M, Beleaga A, Silvestru C, Nicolescu A, Deleanu C, Todasca C & Silvestru A, *Dalton Trans*, (2007) 2187.

30 Selvakumar K, Singh H B, Goel N, Singh U P & Butcher R J, *Chem Eur J*, 18 (2012) 1444.

31 Bondi A, *J Phys Chem*, 68 (1964) 441.

32 Sharma R K, Kedarnath G, Wadawale A, Jain V K & Vishwanadh B, *Inorg Chim Acta*, 365 (2011) 333.

33 Dhau J S, Singh A, Singh A, Sooch B S, Brandao P & Felix V, *J Organome Chem*, 766 (2014) 57.

34 Sousa-Pedrares A, Duran-Carril M L, Romero J, Garcia-Vazquez J A & Sousa A, *Inorg Chim Acta*, 363 (2010) 1212.

35 (a) Han H F, Xu Y, Guo . Q, Zheng Y H, Tong H B & Wei X H, *Wuji Huaxue Xuebao,* 25 (2009) 1073; (b) Niu D Z, Yao L & Zhang Y, *Z Kristallogr-New Cryst Struct*, 230 (2015) 245.

36 Guo Z, Wang Y, Xu Y & Wei X, *IUCr Data*, 2 (2017) x170882 (1-5).

37 Dhau J S, Dhir R, Singh A, Brandao P & Felix V, *Inorg Chim Acta*, 404 (2013) 160.

38 Bhasin K K, Singh J & Singh K N, *Phosphorus, Sulfur, Silicon, Relat Elem*, 177 (2002) 597.

39 Dhau J S, Singh A & Dhir R, *J Organomet Chem*, 696 (2011) 2008.

40 Dhau J S, Singh A, Singh A, Sooch B S, Brandao P & Felix V, *Inorg Chim Acta*, 392 (2012) 335.

41 Gámez J A and Yáñez M, *J Chem Theory Comput*, 7 (2011) 1726.